



# Preparation and Characterization of Thermoplastic Grafted Chitosan Compositions with L-Lactide as Potential Material for 3D Printing

Taisiya Bolkhovskaya<sup>✉, I, \*</sup>  Marina Giricheva<sup>✉, I</sup>  Ivan Lednev<sup>✉, I</sup>  Kristina Apryatina<sup>✉, I</sup>   
Larisa Smirnova<sup>✉, I</sup> 

<sup>1</sup> Chemistry Department, National Research Lobachevsky State University of Nizhny Novgorod, 23 Gagarin Ave, 603022 Nizhny Novgorod, Russia

## Article History

Submitted: November 14, 2024

Accepted: January 08, 2025

Published: January 21, 2025

## Abstract

Chitosan is a natural polysaccharide with excellent biocompatibility and biodegradability, which makes it a promising biomaterial for various biomedical applications. However, its mediocre mechanical characteristics and non-thermoplasticity limit its wider use, since it cannot be melted, which means it cannot be used in 3D printing. In this study, the focus was to overcome this limitation by successfully synthesizing a grafted copolymer of chitosan and L-lactide through a ring-opening polymerization. The resulting copolymer showed melting ability with a melt index of 5 and satisfactory mechanical properties with a tensile strength of 68.3 MPa, which indicates the potential of the copolymer for structural applications. The thermal properties of the copolymer were studied by the differential scanning calorimetry method. In vitro studies indicate that the copolymer is non-toxic to cells and promotes adhesion and proliferation of fibroblasts. The wettability of the copolymer surface was also improved compared to pure polylactide, which increased its cell adhesion for fibroblasts. Overall, this study demonstrates the potential of the grafted chitosan/polylactide copolymer as a biomaterial for biomedical applications.

## Keywords:

chitosan; polylactide; grafted copolymer; biocompatible; thermoplastic; biodegradable

## 1. Introduction

Advanced three-dimensional printing (3DP) technologies have a huge impact on the production of new biomedical instruments and devices [1]. The biggest advantage of 3DP technologies is the absence of a significant time interval between the design and final production stages, which is typical for other technologies in the same field [2]. This allows manufacturers to create products for specific patients that precisely meet individual requirements [3].

The production of thin filaments by melting in an extruder is widely recognized as a very flexible and inexpensive production process for the development of indi-

vidual scaffolds from thermoplastic biomaterials [4]. 3DP technology allows the creation of biomimetic scaffolds from biocompatible low-melting polymers such as polycaprolactone and polylactide (PLA), mixtures of several materials, as well as soft biomaterials such as hydrated gels [5]. The selected biomaterials should not only promote the regeneration of the patient's tissues and guarantee the desired mechanical characteristics [6], but also have antibacterial properties [7]. For example, biocompatible and biodegradable [8] PLA-based polymers are used for FFF printing because of their high rheological characteristics and because they can decompose over time in the human body [9].

\* Corresponding Author:

Taisiya Bolkhovskaya, Chemistry Department, National Research Lobachevsky State University of Nizhny Novgorod, 23 Gagarin Ave, 603022 Nizhny Novgorod, Russia, bolkhovskiyat@gmail.com



© 2025 Copyright by the Authors.

Licensed as an open access article using a CC BY 4.0 license.

Furthermore, PLA production is carried out from renewable resources, often from silage-forming crops, which makes it possible to consider PLA an environmentally friendly material [10]. The polymer has fine mechanical strength, as mentioned above, (50–60 MPa), which can be adjusted by changing the molecular weight and the ratio of L-lactic acid to D-lactic acid [11].

PLA has established itself as a biopolymer with broad functionality in the field of biomedicine [12–14]. It can be used in 3DP for the design and synthesis of implants, which expands the use of PLA specifically in bone engineering [15]. However, despite its biocompatibility, PLA has the disadvantage of lacking functional groups that provide cellular adhesion to the surface, which leads to the fact that the material does not stimulate cell growth. Adding the fact, that PLA's surface is hydrophobic by nature, it is reasonable to add biofunctionality to scaffolds, printed from PLA. For this reason, it is necessary to modify the PLA [16,17].

Biocompatible and biodegradable chitosan is considered the optimal polymer to combine with PLA [18]. Chitosan is obtained from chitin, which is one of the most widespread polysaccharides in nature. It can be found in the cell walls of fungi [19], as a component of the arthropod exoskeleton, in organisms of various worms and coelenterates, in marine sponges [20]. Chitosan has a number of properties valuable for medicine—biocompatibility [21], nontoxicity, antioxidant and antimicrobial activity [22], the ability to film formation, chemical, thermal and other types of modification [23], as well as complete biodegradability [24].

With all these advantages, pure chitosan is fragile and demonstrates low mechanical characteristics. Consequently, it is not used in its pure form for applications such as bone engineering, but is subject to modifications [23]. In order to change the characteristics of chitosan, modification with polyesters is used, among which PLA is a popular choice due to its availability [25].

The combination of chitosan and PLA provides hydrophilicity of the scaffold surface, high mechanical strength and conditions for fibroblast growth [26]. The authors [27] combined polymers in a solvent with subsequent removal during the formation of film samples and leaching for the purpose of applying chitosan to PLA. This approach resulted in enhanced cellular adhesion and the proliferation of osteoblasts. In [28], the authors analyzed the cellular growth of cells and their apoptosis, as well as studied the cytocompatibility and antibacterial properties of the resulting mixture.

In [29], chitosan was combined with PLA by the 3DP method. However, as in many works on this topic, scientists have concluded that an increase in the content of chitosan

in a printed sample above 1% leads to a significant deterioration in the mechanical properties of the scaffold and, in principle, complicates the printing process itself.

Scientists mixed chitosan with PLA, dissolving the first polymer in water, and the second in chloroform, and then obtaining an emulsion. Samples were selected for the study [30]:

The mechanical characteristics of the samples significantly depended on the ratio of the components, reaching the maximum value for a composition with the addition of 50% PA (tensile strength— $72.1 \pm 8.2$  MPa and deformation  $10.3 \pm 1.9\%$ ).

In [31], chitosan/PLA copolymers were obtained for the chitosan: PLA 80:20 and chitosan: PLA 50:50, containing 82 wt. % and 55 wt. % chitosan, respectively. Nanomechanical studies have shown that a copolymer with a higher content of chitosan has a larger Young's modulus, reduced values of modulus of elasticity and hardness, compared with the second sample. In vitro studies have shown that MC3T3-E1 cells showed strong adhesion to films with a high content of CTP.

In [32], PLA, keratin and chitosan were used to manufacture scaffolds from polymer composites suitable for 3D printing. Keratin and chitosan, used as a reinforcing agent in PLA, improve the thermomechanical properties and biocompatibility of the samples in this case.

In [33], composite scaffolds from chitosan with open-pore PLA were obtained. In this case, the PLA was a matrix on which the copolymer chitosan/PLA was fixed in a 1:1 ratio as a dispersed biopolymer phase. At the same time, the obtained samples were more flexible under compression, and also demonstrated hydrolytic stability, unlike chitosan/PLA composites, which were not modified with a copolymer.

In [34], the copolymer chitosan/PLA/PEG (polyethylene glycol) was used for hydrophilic encapsulation of nanoparticles in medicines. There was a significant sealing of bonds between the material sites and hydrophilic drugs, which led to improved encapsulation of therapeutic molecules.

It should be noted that in these studies, chitosan/PLA compositions with different component ratios were investigated, and satisfactory results in uniformity, strength and fusibility of the samples were obtained only with a large excess of polyester. At the same time, more satisfactory data on biocompatibility and biodegradability suggest an increased (more than 25%) content of chitosan. In some cases, samples with comparable amounts of polymers were obtained (chitosan: PLA 1:1), but the method of preparation involved the use of solvents incompatible with the use of the obtained samples in the human body.

Further, almost no studies have provided data on samples melting, which is crucial for 3DP.

So, despite the great potential of chitosan/PLA composites for biomedical applications, not many studies on 3DP from such materials have been published, since there is no optimal way to obtain a composite with the ability to melt and the qualitative ratio of the components.

Previous efforts to develop 3D-printable compositions of chitosan and PLA have faced significant challenges, primarily due to the inherent immiscibility of these two polymers. PLA is predominantly soluble in organic solvents, whereas chitosan dissolves in aqueous acidic solutions. When attempting to combine these polymers, one typically encounters conditions in which at least one of the components is placed in an incompatible solvent environment. This typically results in the formation of a suspension rather than a true solution. As a result, the mixture often constitutes a mechanical blend rather than a genuine copolymer or homogeneously modified material. Such blends exhibit poor interfacial compatibility and lack the necessary structural cohesion, which adversely affects their thermoplastic properties. Specifically, mixtures with higher chitosan content fail to achieve melt processability due to phase separation and the absence of synergistic interactions between the polymers.

Consequently, previous studies have predominantly resorted to formulations with minimal chitosan content (e.g., ~5%), ensuring sufficient PLA dominance to maintain melting behavior. However, low chitosan concentrations severely limit the functional contributions of chitosan, such as antimicrobial activity and biocompatibility. Achieving higher chitosan content (e.g., ~25% and more) remains critical to unlocking these functionalities, necessitating innovative strategies to enhance compatibility and processability.

The purpose of the work is to obtain homogeneous grafted melting compositions of chitosan/PLA and characterize its properties.

## 2. Materials and Methods

### 2.1. Materials

In this study following materials were used: chitosan with viscosity average molecular weight ( $M_{\eta}$ )  $200 \times 10^3$  and degree of deacetylation 82% (source—crab, LLC Bio-progress, Moscow, Russia); L-lactide (L-LA) (ACROS Organics, Geel, Belgium); acetic acid (99%, Khimreaktiv, Moscow, Russia); DMSO (chemically pure, Khimreaktiv, Moscow, Russia).

The average molecular weight of chitosan was determined by viscosimetry. Measurements were carried out

on an Ubbelohde viscometer at 25 °C in a 2% solution of acetic acid with the chitosan concentration of 0.1%. The viscosity average molecular weight was calculated using the Mark–Kuhn–Houwink equation  $[\eta] = k \cdot M_{\eta}^{\alpha}$ , where  $k = 3.41 \times 10^{-5}$  and  $\alpha = 1.02$  [35]. The degree of deacetylation of chitosan was determined by potentiometric titration of its 0.1% solutions in a 0.1 N HCl solution with NaOH solution (0.1 N) using pH meter (FiveEasy Plus pH meter FP20-Std-Kit, Mettler Toledo, Columbus, OH, USA).

### 2.2. Preparation of Chitosan Solutions

To obtain a solution in DMSO, chitosan was suspended in a solvent, then hydroxyacids (citric, amber, malic, lactic) were added and mixed until a transparent solution was obtained. The composition of the mixture: 3% chitosan, 1.5% hydroxyacid, DMSO.

The selection of hydroxy acids (citric, amber, malic, and lactic) was based on their established compatibility with chitosan and their ability to influence the material's properties, such as improving solubility and enhancing the grafting process. These hydroxy acids were chosen for their widespread use in polymer chemistry, where they contribute to desirable attributes such as biocompatibility and biodegradability.

### 2.3. Synthesis of Grafted Chitosan Copolymer with L-Lactide

The synthesis was carried out in small volumes (150–300 mL) for even heating and mixing of all components. DMSO was placed in a three-necked flask and purged with an inert gas (argon) in order to purify the reaction medium from air. Then the solvent was heated to the synthesis temperature (100 °C) and thermostated for an hour with constant stirring.

Chitosan powder was added to the solvent and mixed until a suspension was obtained. Then hydroxyacids were added and left under constant heating and stirring until a solution was obtained.

The chitosan solution in DMSO was repeatedly purged with argon, after which the monomer (L-lactide) was added while stirring to produce a chitosan/L-lactide solution. Immediately after L-lactide was added, cycle opening catalysts (isopropyl alcohol) were introduced into the system. These are standard cocatalysts, which are also used in the homopolymerization of L-lactide together with tin octate. Then, after purging the system with argon, it was sealed. The synthesis was carried out for 17 h in an inert gas atmosphere.

Composition of the synthesis mixture: 1.5% chitosan, 6% L-lactide, 0.75% hydroxyacid, and a catalyst.

## 2.4. The Effectiveness of the Synthesis Method

To characterize the process, the following values were calculated: yield by weight ( $\eta$ ), the degree of grafting (GD) and the effectiveness of grafting (GE).

As a result, the yield by weight was 82%, with a grafting efficiency of 100%. Unlike the yield of the product, which is unlikely to be 100% in real conditions, the effectiveness of grafting indicates what percentage of the polymerized substance went to form a copolymer. Since no homopolymer is formed during the synthesis process, the resulting value of 100% is quite realistic. The effectiveness of grafting was 229%, since after the primary attachment of the L- grafting molecule to the chitosan, the growth of the polylactide chain occurs.

## 2.5. Obtaining Film and Powder Samples

Powdered samples of grafted compositions were sedimented from the solution using their insolubility in isopropanol. After sedimentation from the solution, the sediment was vacuum-dried to a constant mass and shredded with liquid nitrogen into a powder.

The films were obtained by watering on a dacron, silicone, glass and teflon base. The solutions were degassed and dried under conditions of even evaporation of the solvent during the day at a temperature of 65 °C to a constant mass.

## 2.6. IR Spectroscopy

The IR spectrum of powdered samples was obtained in petroleum jelly oil. A small amount of the powdered sample was ground with oil, then the mixture was placed between sodium chloride glasses and fixed in an IRPrestige-21 IR spectrometer.

Thin film samples were also placed between sodium chloride glasses and fixed in an IRPrestige-21 IR spectrometer.

## 2.7. Mechanical Properties

The physical and mechanical characteristics (tensile strength and elongation at break) of the material were determined on a Roell/Zwick Z005 breaking machine in accordance with ASTM D 882 [36]. The tests were carried out at a tensile rate of 10 mm/min on samples with a thickness of  $60 \pm 5$  microns in the form of rectangles with a width of 10 mm. At least 10 measurements were carried out for each film composition.

## 2.8. Thermophysical Properties

The thermophysical properties of the samples were studied by differential scanning calorimetry (DSC) on the DSC204F1 Phoenix device (NetzschGerätebau, Germany).

Powders were used as test samples. A 30 mg powder sample was placed in one of the crucibles of the device, the second comparison crucible was left empty.

Next, the sample was heated at a rate of 2 °C per minute, the measurements of the samples were carried out in an argon atmosphere.

## 2.9. Melt Flow Index (MFI)

The MFI is determined according to ASTM D1238 [37] by the formula:

$$MFI = 600 \cdot \frac{m}{t}$$

where 600 is the standard time equal to 600 s (10 min);  $m$  is the average mass of the extruded segments, g;  $t$  is the time interval between two consecutive sections of segments.

The device Melt flow index tester tm2101-t5 Shanghai Goldsu Industrial Co., Ltd was used, with standard 6 capillaries made of hardened steel with a length of 8.0 mm and an internal diameter of 2.095 mm. The pressure on the polymer is transmitted using a steel piston 3 with a guide head. The extrusion chamber is heated by a heater up to 400 °C.

A temperature of 170 °C was set in the extrusion chamber for samples containing PLA. The weight of the suspension was 5 g, the weight of the load was 3 kg.

## 2.10. Investigation of the Biocompatibility

The growth of cells on the surface of the film was studied during the cultivation of human fibroblasts of the hTERT BJ-5ta cell line. The films of the material, after sterilization by autoclaving at a temperature of 110 °C, were placed in the wells of a cell culture tablet and filled with 500  $\mu$ L of DMEM medium. The cells were seeded onto the surface of a film with a density of  $1.6 \times 10^5/\text{cm}^2$  and cultured for 24 h.

Cell imaging and viability were assessed by luminescent microscopy.  $2 \times 10^{-4}$  mas were used as a dye for staining fibroblasts. A  $2 \times 10^{-4}$  wt. % solution of acridine orange in a phosphate buffer. This dye selectively interacts with DNA and RNA located in the nucleus and mitochondria of the cell, respectively, by intercalation or electrostatic attraction. This allowed to assess the general condition of cells—activity, proliferation and apoptosis.

Microsampling of the films was performed on an Olympus X71 inverter microscope (Japan/Germany) using a “green” filter (emission 510–555 nm, excitation 460–495 nm), which makes it possible to visualize the green color of the nucleus of living cells.

A cytotoxicity scale was used to qualitatively assess the cytotoxicity of the studied scaffolds (Table 1).

## 2.1.1. Contact Angle Measurements

Contact angles of wettability were measured using 1  $\mu\text{L}$  of water droplets as a testing liquid.

To analyze the wettability of the film samples, a Levenhuk DTX 30 Digital microscope was used. The samples were prepared for analysis by cutting small square pieces ( $2 \times 2$  cm) from various sections of the films. The samples were placed on a substrate and secured with double-sided adhesive tape, then analyzed.

All measurements were carried out at a temperature of 23  $^{\circ}\text{C}$ . To analyze the static contact angle, a drop of liquid with a volume of 1  $\mu\text{L}$  was placed on the surface of the sample and the contact angle was measured after 200 s. The static contact angle was calculated by averaging five values.

## 3. Results and Discussion

### 3.1. Synthesis of Grafted Copolymer Chitosan/PLA

To simplify the reaction and increase the yield of the product, chitosan was pre-dissolved in DMSO, unlike other known combination attempts, where chitosan was suspended but not dissolved in an organic medium.

There was a possibility that L-LA would homopolymerize without interacting with chitosan. To check for the presence of the L-LA homopolymer, the aliquot of the solution was treated with isopropanol, in which both chitosan and PLA are insoluble. The resulting precipitate was subjected to THF extraction for three days with constant stirring, since THF dissolves PLA (and possibly copolymer), but does not dissolve chitosan.

After extraction, the powder that did not dissolve in THF was separated from the solvent. The solvent was then tested for the presence of dissolved polymers by adding water drop by drop. PLA is insoluble in water, and instantly precipitates in its presence. Chitosan is also insoluble in water with a neutral pH value of the medium, and therefore the insolubility of the copolymer in water is assumed. However, after three days of extraction, no polymers could be sedimented from THF under the action of water. Then the THF was dried, and after drying it did not leave any sediment.

The IR spectrum of the solvent was also obtained, where the bands  $1564.28\text{ cm}^{-1}$  and  $1754.27\text{ cm}^{-1}$  (characteristic for chitosan and PLA) were not detected.

The experiment was repeated with chloroform, another selective solvent of PLA. The result of the experiment was similar to the first one. It was concluded that no formation of the PLA homopolymer occurs during the reaction, and L-LA is partially grafted onto the chitosan, forming a copolymer, and partially remains in solution as a monomer.

This conclusion is confirmed by the following facts:

- there is no homopolymer in the solution after synthesis
- a copolymer is present in the solution, the yield by weight is 88%
- thus, the remaining monomer did not polymerize and remained in solution

### 3.2. The Reaction of Obtaining the Grafted Copolymer Chitosan/PLA

During the synthesis of the grafted copolymer chitosan/PLA, a scheme was proposed according to which the reaction presumably proceeds (Figure 1).

According to the proposed scheme, the copolymerization process includes:

1. L-LA ring opening: Initially, L-LA (cyclic ester) undergoes ring opening in the presence of a nucleophile. In this case, the nucleophile is the  $\text{NH}_2$  group of the polysaccharide. An unshared pair of electrons of the nitrogen atom attacks the electrophilic carbon atom of the carbonyl group

**Table 1:** A cytotoxicity scale.

A Cytotoxicity Scale	The Number of Dead Cells in the Culture, %	Interpretation
0	0–10%	Not cytotoxic
1	10–20%	Mild cytotoxicity
2	20–30%	Average cytotoxicity
3	over 30%	Significant cytotoxicity



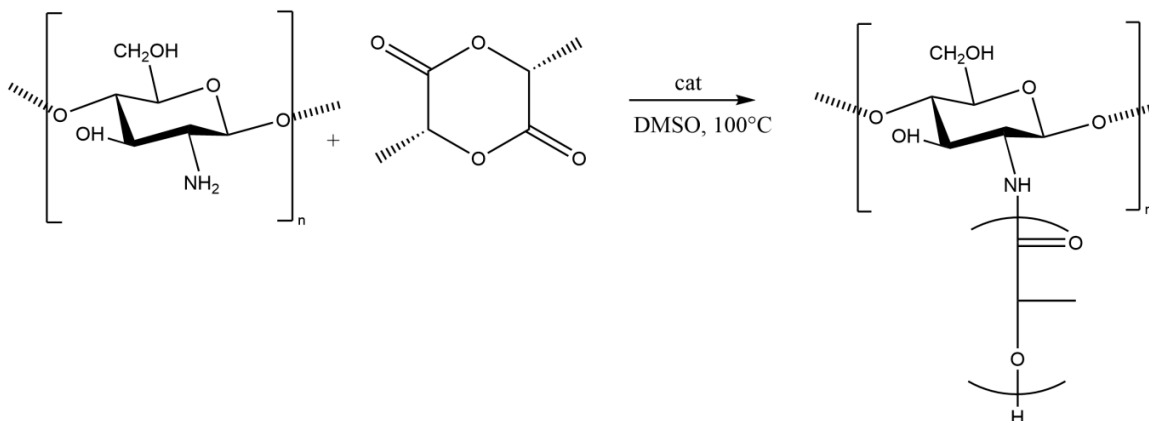


**Figure 1:** Reaction scheme for the production of a grafted copolymer chitosan/PLA.

of L-LA, disrupting the cyclic structure. This nucleophilic attack leads to the formation of an intermediate.

2. Substitution of hydrogen with L-LA: when the L-LA ring is opened, the nitrogen atom of the NH<sub>2</sub> group forms a covalent bond with one of the carbon atoms in the lactide molecule, effectively replacing the hydrogen atom originally attached to the nitrogen atom. This leads to the addition of the lactide monomer to the polysaccharide chain.

3. Polymerization of L-LA: after the initial substitution reaction, additional lactide monomers undergo similar ring opening reactions, sequentially joining the growing polymer chain attached to the polysaccharide. As more lactide monomers are added, the polymer chain lengthens, which leads to the formation of a polymer chain consisting of lactide.

It is important to note why in the proposed reaction scheme for obtaining a grafted chitosan copolymer with L-LA, substitution occurs in the amino group and not in the hydroxyl group. The NH<sub>2</sub> group is usually more nucleophilic than the OH group. This higher nucleophilicity is due to the greater availability of an unshared pair of electrons in nitrogen compared to oxygen. Consequently, the NH<sub>2</sub> group is more likely to participate in nucleophilic attacks. Kinetically, if the reaction rate for the NH<sub>2</sub> group is higher due to its higher nucleophilicity or other kinetic factors, the substitution reaction will predominantly occur at this location.

### 3.3. The Rate of Obtaining the Grafted Copolymer Chitosan/PLA

The rate of the process of obtaining the grafted copolymer chitosan/PLA was investigated by the weight method.

According to the data obtained (Figure 2), (Figure 3) 17 h after the start of synthesis, the conversion depth of the

monomer ceases to change. Thus, the optimal synthesis duration is 17 h.

### 3.4. IR Spectroscopy

To confirm the composition of the obtained copolymer, IR spectroscopy of chitosan/PLA samples was performed (Figure 4).

On the IR spectrum of the copolymer, one can see:

- 1157 cm<sup>-1</sup> is a CO stretching band associated with fluctuations in the CO bond in the ester group of PLA
- 1546 cm<sup>-1</sup>. Deformation vibrations of NH in amino groups of chitosan
- 1667 cm<sup>-1</sup>—vibrations of the carbonyl section (C=O) in the primary amide bond (CONH<sub>2</sub>) of deacetylated chitosan units
- 1747 cm<sup>-1</sup> is a band of valence vibrations C=O, associated with valence vibrations of the carbonyl group in the ester bond of PLA
- 2924 cm<sup>-1</sup>—Two bands side by side, refer to asymmetric and symmetric valence vibrations of CH groups in the PLA

Thus, the presence of bands characteristic of both chitosan and PLA in the copolymer is obvious. It is worth noting that the bands up to 2000 cm<sup>-1</sup> are located with almost no shift relative to the bands of the starting substances.

However, the bands located after 2000 cm<sup>-1</sup> do not completely coincide with the starting substances. A wide band of 3400 cm<sup>-1</sup> valence vibrations of hydroxyl chitosan groups is not visible. In pure chitosan, OH groups are likely involved in extensive hydrogen bonding with neighboring hydroxyl groups or other functional groups within polymer chains. This strong hydrogen bond limits the vibrational freedom of the OH groups, which leads to a distinct peak at 3400 cm<sup>-1</sup>. In the copolymer, the presence of another type of polymer chains along with

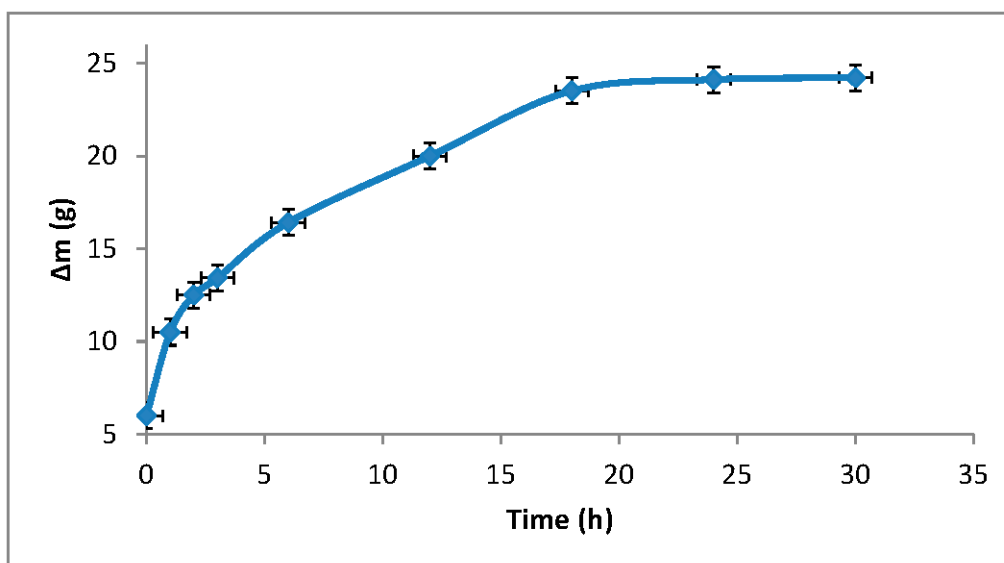


**Figure 2:** Dependence of the mass of the copolymer formed on the synthesis time.

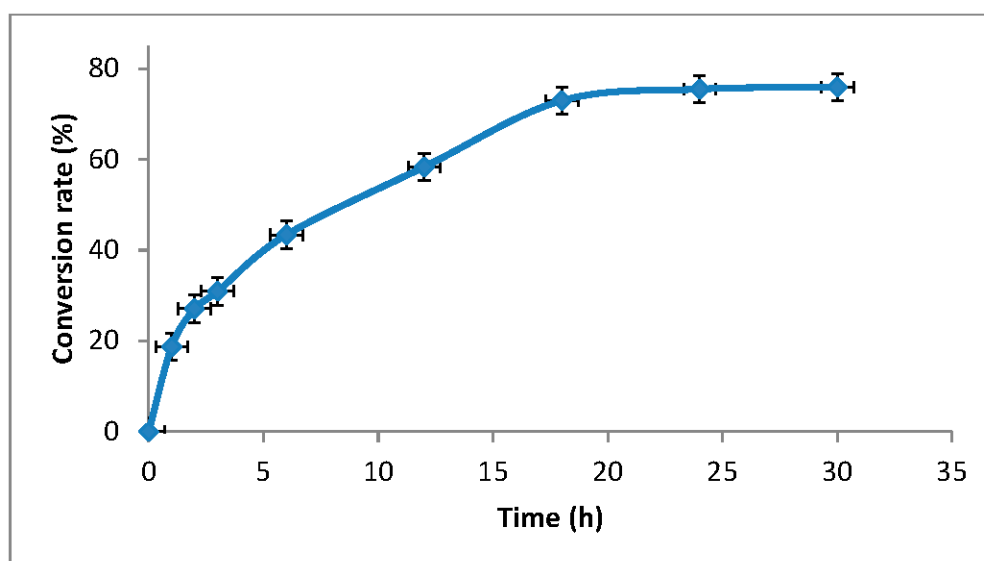


**Figure 3:** Dependence of monomer conversion on synthesis time.

chitosan can destroy this extensive network of hydrogen bonds. Weaker hydrogen bonds can lead to a broadening and decrease in peak intensity, which can potentially lead to the disappearance of the  $3400\text{ cm}^{-1}$  band in background noise.

### 3.5. Mechanical Properties

Although the main focus of this study was to obtain a melting material with satisfactory biocompatibility, strength properties are just as important for this copolymer. So, it

is important to characterize physical and mechanical properties of a chitosan/PLA grafted copolymer.

The results of measuring the strength properties of films obtained on the basis of grafted compositions with different component ratios are presented in [Table 2](#).

[Figure 5](#) shows the L-LA content in experimental samples along the abscissa axis. Strength values for chitosan and PLA can be found in [Table 1](#).

As can be seen from the results of the study of mechanical properties ([Figure 5](#)), when adding 24–68% L-lactide to chitosan, the mechanical strength values of the samples are between the strength values of individual

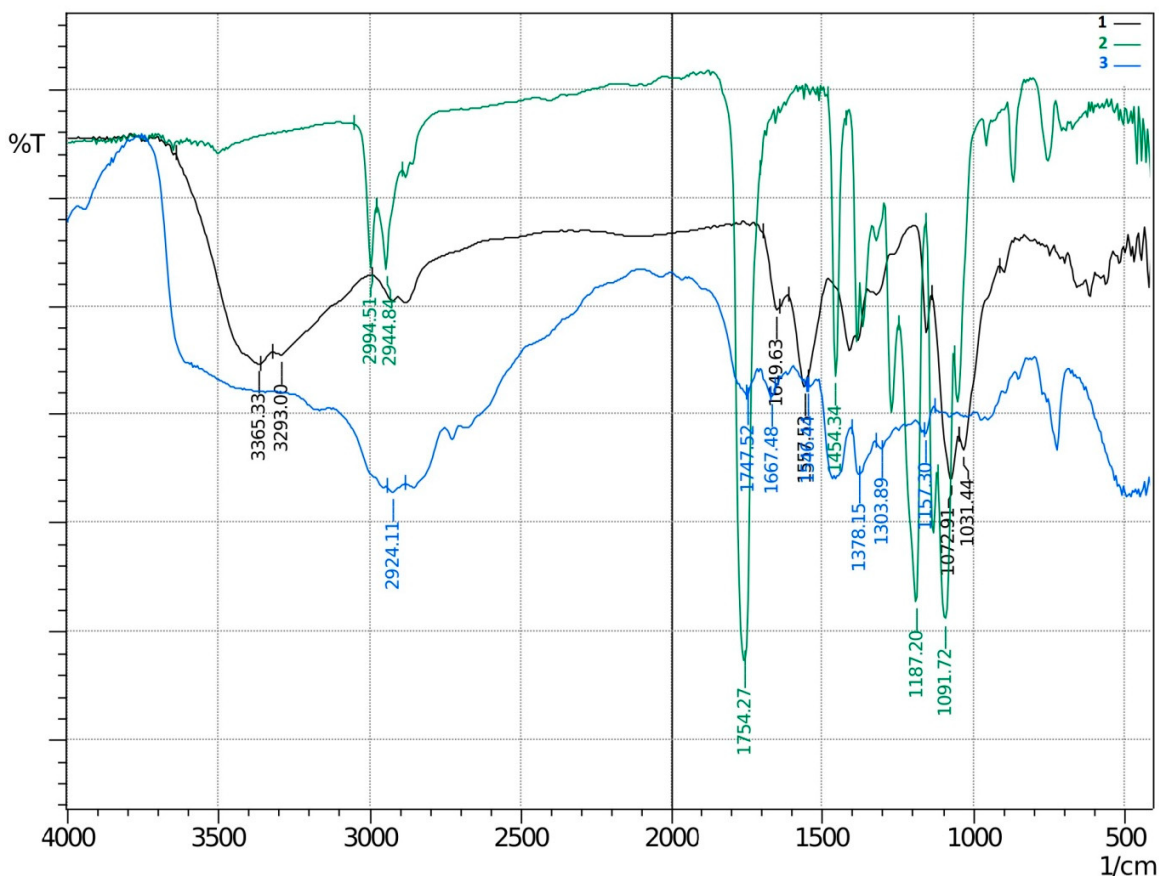


**Figure 4:** IR spectrum of 1—chitosan, 2—PLA, 3—grafted chitosan/PLA.

components (19–58 MPa). However, the introduction of more than 68% L-LA increases the mechanical strength and elasticity of the material so much that it exceeds the strength values of both initial components (68.3 MPa for the composition of chitosan: LA 1:3).

It can be assumed that this is explained by the peculiarities of the intermolecular structure of the composition: covalent bonds formed during copolymerization provide high strength characteristics of the polymer. Grafted chains can act as “spacers”, pushing the chitosan chains apart and increasing the free volume inside the copolymer, which leads to higher deformation properties.

Probably, when the proportion of polyester is increased to 90–95%, the highest values of mechanical characteristics can be obtained, up to 100 MPa. However, it is important to note that the addition of chitosan is key to creating a biocompatible material. As will be shown below, with a high content of chitosan, film samples of the composition provide high cellular adhesion and promote the growth of fibroblast cells. The addition of chitosan reduces the risk of inflammatory reactions during the enzymatic decomposition of polyester to lactic acid.

Thus, it is reasonable to introduce the maximum allowable amount of chitosan into the composition, so that high mechanical characteristics are preserved, which still provides high biocompatibility. This is a sample with a ratio of components chitosan: PLA 1:3. Thus, it was the sample with this ratio of components chitosan: PLA 1:3 that was used for further research as the most successful one.

### 3.6. Thermophysical Properties

To characterize the thermophysical properties of the samples, a DSC analysis was performed.

Chitosan, as a non-thermoplastic non-crystalline polymer, does not show melting (Figure 6). There is also no glass transition on its curve. First of all, a smooth rise in the graph up to 230 °C, corresponding to the endothermic process, but not glass transition or melting has been observed. It can be assumed that this is due to the rupture of hydrogen bonds formed by the hydroxyl groups of the polymer. It is also likely that a gradual increase may correspond to an amorphous transition (for example, segmen-



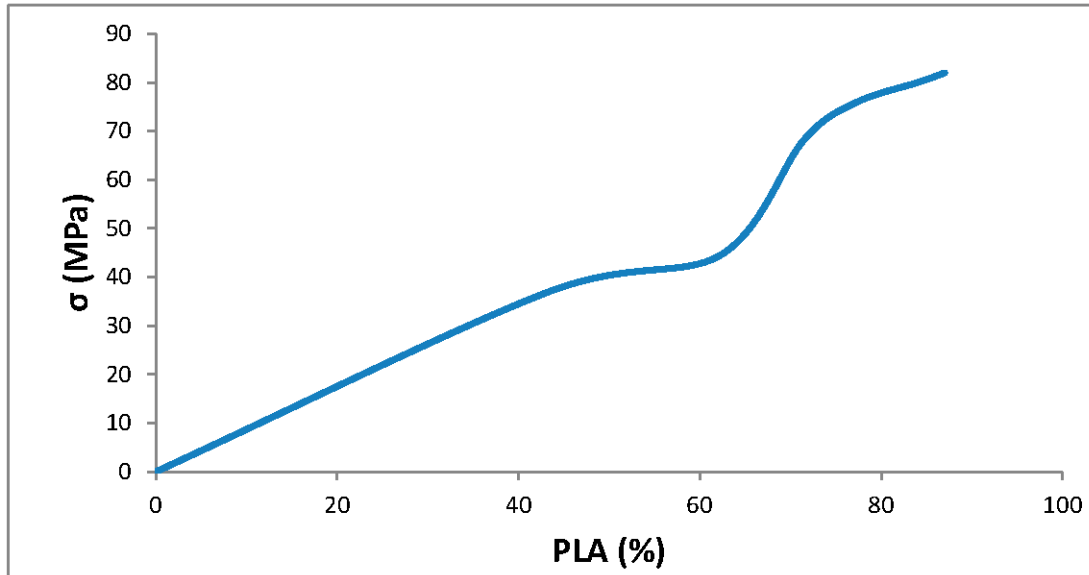


**Figure 5:** Deformation curve of a grafted chitosan/PLA film.

tal movement, relaxation). At a temperature of 260 °C, an exothermic process corresponding to the decomposition of amine units can be observed.

Now, consider the curve corresponding to the PLA. The exothermic peak at 60 °C corresponds to cold crystallization. As can be seen from the DSC curve, this peak is very small, which proves that this PLA is a highly crystalline and highly ordered polymer. The endothermic peak at 180 °C represents the melting of crystallites. The second endothermic rise, starting at 280 °C, indicates the beginning of thermal decomposition of the PLA. At such elevated temperatures, polymer chains begin to break down, which leads to heat absorption (an endothermic process).

When comparing the DSC curve of the grafted composition of chitosan: PLA 1:3 (Figure 6) with the curves of the initial polymers, it can be seen that the melting peak does not appear as clearly as on the PLA curve. Nevertheless, the endothermic process is clearly visible, starting at 140 °C. This transition (or a combination of transitions) is

too blurred to be able to claim that it is melting, and that the grafted copolymer melts.

It can be assumed that the transition at 140 °C is a glass transition that occurs due to chitosan in the composition of the copolymer (despite the fact that there is no glass transition visible on the DSC of pure chitosan). Glass transition is generally characteristic of chitosan, not PLA, but it does not always manifest itself depending on the degree of deacetylation, molecular weight and the method of processing the polymer. Since the chitosan was subjected to additional processing during the preparation of the copolymer, this could lead to the manifestation of glass transition on the DSC curve unlike the DSC curve of pure chitosan.

Further endothermic rise, which is a blurred peak, can be attributed to melting at 210 °C. It is quite logical that the melting has shifted to a region of higher temperatures compared to the melting of pure PLA, since chitosan, which is part of the copolymer, does not melt. In this case, the copoly-

**Table 2:** Mechanical characteristics of film samples of grafted chitosan/PLA compositions.

Composition	Tensile Strength, $\sigma$ (MPa)	Elongation at Break, $\varepsilon$ (%)
Chitosan	$19.4 \pm 0.8$	$1.4 \pm 0.1$
PLA	$55.8 \pm 2.6$	$35.1 \pm 1.8$
Grafted Chitosan: PLA 1:1	$36.9 \pm 1.3$	$13.6 \pm 0.4$
Grafted Chitosan: PLA 1:2	$44.5 \pm 2.2$	$23.2 \pm 2.0$
Grafted Chitosan: PLA 1:3	$68.3 \pm 1.9$	$29.9 \pm 2.3$
Grafted Chitosan: PLA 1:4	$75.9 \pm 1.5$	$35.9 \pm 1.6$

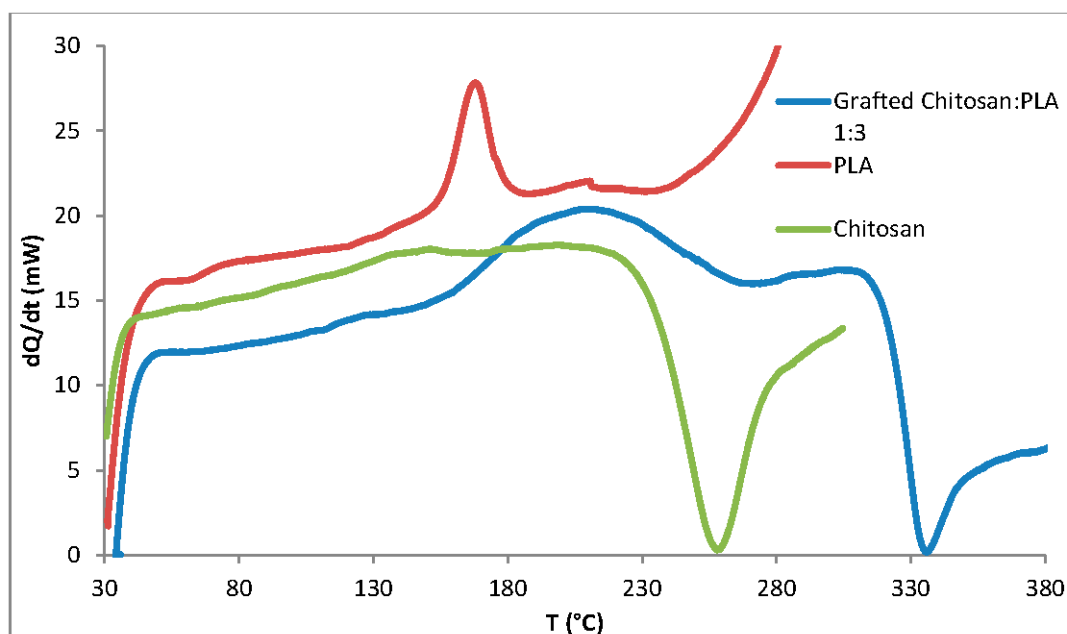


**Figure 6:** DSC curves of samples. The exoeffect is directed downwards.

mer is not a mechanical mixture, probably the bonds formed between chitosan and L-LA prevent melting.

The onset of decomposition of the copolymer can be observed at 335 °C, which exceeds the values of the decomposition temperatures of individual components.

### 3.7. Melt Index

As mentioned earlier, when creating a chitosan /PLA copolymer, the key characteristic is the ability to melt so that the resulting material can be processed by molding. To quantify this characteristic, the melt flow index was measured (Table 3).

The very fact of thermoplasticity is confirmed by the availability of the flow index for the polymer. If the polymer is thermoplastic to some extent, it is possible to measure the flow index. If the polymer is not thermoplastic, the flow index cannot be measured at all. It is important to note that the properties of different polymers should be compared under the same conditions so that their flow index values can be comparable.

**Table 3:** Flow index values for experimental samples.

Sample	Flow Index, g/10 min
Chitosan	-
PLA	10
Grafted chitosan: PLA 1:3	5

As it was shown in the literature review, in other studies, small amounts of chitosan (up to 4%) were introduced into the composition of chitosan/polyester, which were insufficient to ensure the biocompatibility of samples. When trying to introduce large amounts of chitosan, researchers were faced with the impossibility of molding or 3D printing from such compositions. Thus, in [38] the maximum content of chitosan is 2%, in [25]—4% of chitosan, in [29]—1% of chitosan. It is also important to emphasize that chitosan, as a non-thermoplastic polymer, does not have a flow index. In this work, it was possible to obtain a material containing 25% chitosan, which, nevertheless, melts.

### 3.8. Biocompatibility Studies

In vitro studies of film samples on adhesion and proliferation of fibroblast cells hTERT BJ-5ta cell line were carried out. Film samples were used for the study:

- Pure chitosan
- Pure PLA
- Grafted chitosan: PLA 1:3

It has been established that film samples (except for films made of pure PLA) are non-toxic to cells and have sufficient adhesive properties for the attachment and development of fibroblast cells on their surface (Figure 7).

Also, it was shown that the films of chitosan and grafted copolymer do not have cytotoxic properties

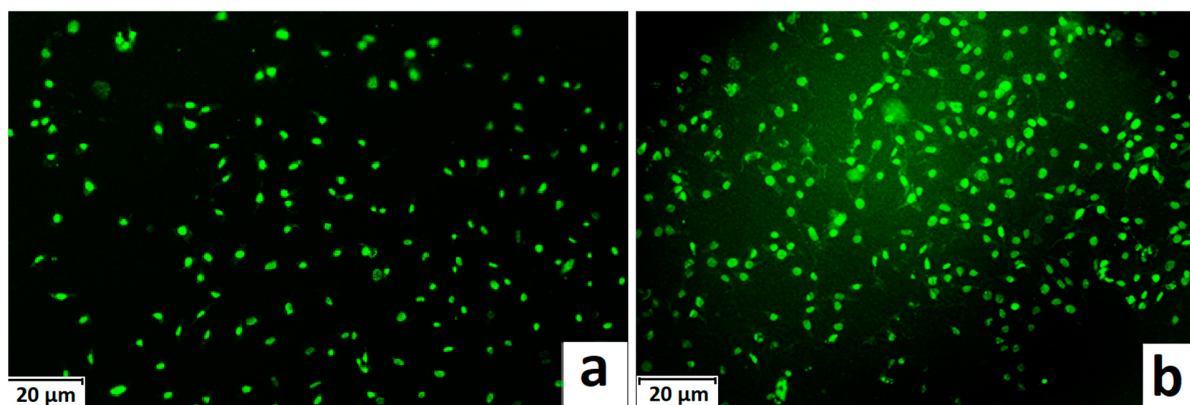


**Figure 7:** Photographs of films of (a) the grafted chitosan:PLA 1:3 and (b) pure chitosan after 24 h of cell incubation.

(cytotoxicity—0 points), therefore they can be used for further development of scaffolds (Figure 8).

Chitosan promotes adhesion and proliferation of fibroblast cells, and its hydrophilic surface ensures high adhesion of these very cells. Films based on this polymer show an excellent distribution of fibroblast cells on the surface. It is this characteristic that allows chitosan to be used to “enhance” PLA. PLA is also biocompatible and biodegradable, but its hydrophobic surface prevents the attachment and spread of cells, and the release of lactic acid during hydrolysis of PLA is also a problem. So, if chitosan can be called “strictly positive” for cells, then PLA will be “neutral”.

Films based on the grafted chitosan/PLA are characterized by a uniform distribution of fibroblasts on the surface. Despite the fact that cell growth on films of the grafted composition is less pronounced than on films made of pure chitosan, the samples in any case demonstrate good biocompatibility. Thus, even with the addition of 25% chitosan to the composition, it is possible to achieve sufficient modification for high cell adhesion, which is a key factor for the use of the material in biomedical applications.

### 3.9. Wettability Study

As mentioned earlier, the hydrophilic surface of chitosan promotes the attachment of fibroblast cells, while the hydrophobic surface of PLA prevents this. In order to study the surface characteristics of the grafted chitosan/PLA copolymer more deeply, the wettability of the samples was evaluated after biocompatibility (Figure 9).

Pure chitosan film (49.56°): such a low contact angle indicates the hydrophilic nature of chitosan. The presence of hydroxyl (-OH) and amino (-NH<sub>2</sub>) groups in its

structure makes it possible to form strong hydrogen bonds with water, contributing to wetting.

Pure PLA film (90°): The high contact angle confirms the hydrophobic character of the PLA. Methyl groups in its structure create a water-repellent surface.

Grafted chitosan/PLA film (68.85°): The contact angle of the copolymer is between the contact angles of pure chitosan and PLA, which demonstrates the synergistic effect of their combination. As it could be seen, the main task is to make the surface of the copolymer wettable, which is successfully solved by adding 25% chitosan to the PLA.

## 4. Conclusions

A grafted copolymer of chitosan/PLA in ratio chitosan:PLA 1:3 with good mechanical properties, high melt index and biocompatibility has been successfully synthesized. The resulting thermoplastic material contains 25–30% chitosan and 70–75% PLA. The synergistic effect of strength and biocompatibility inherent in individual substances is achieved. The copolymer demonstrated potential for biomedical applications since it supported cell adhesion and proliferation and had improved surface wettability compared to pure PLA.

The material shows great promise for use in the production of tissue-substituting implants, particularly with 2D and 3D printing methods, which offer high precision and customizability for biomedical applications. However, further research is needed to explore the scalability of the synthesis process, as well as in vivo studies. Additionally, while the material’s biocompatibility has been demonstrated, more extensive testing in various tissue types and conditions would be valuable. Addressing these aspects could help optimize the material for broader

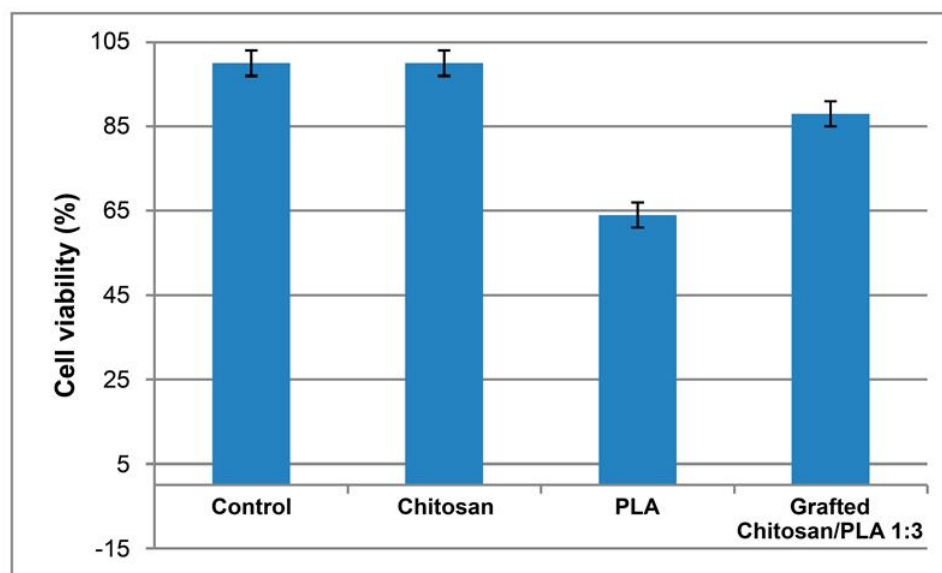


**Figure 8:** Assessment of cell viability of primary fibroblast cultures.

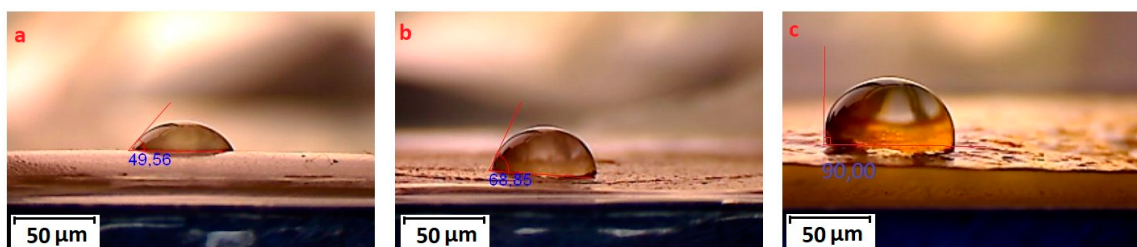


**Figure 9:** Photographs of water droplets on films made of (a) pure chitosan, (b) grafted chitosan/PLA, (c) pure PLA.

applications, such as personalized medicine or advanced regenerative therapies.

## 5. List of Abbreviations

3DP: three-dimensional printing  
FFF: Fused Filament Fabrication  
PLA: polylactide  
PEG: polyethylene glycol  
L-LA: L-lactide  
DMSO: dimethyl Sulfoxide  
GD: the degree of grafting  
GE: the effectiveness of grafting  
IR: infrared  
DSC: differential scanning calorimetry  
MFI: melt flow index  
DMEM: Dulbecco's modified Eagle's medium  
THF: Tetrahydrofuran

## Author Contributions

Conceptualization, validation, data curation, supervision, L.S. and I.L.; formal analysis, investigation, M.G.; methodology, formal analysis, investigation, writing—original draft, project administration, funding acquisition, B.T.; writing—review & editing, K.A.

## Availability of Data and Materials

The data underlying this study are available in the published article.

## Ethics Committee Approval and Consent to Participate

This study does not include experiments that require approval from an ethics committee. All experiments were conducted in vitro, which does not necessitate such permissions.

## Consent for Publication

Not applicable.

## Conflict of Interest

The authors declare no conflicts of interest regarding this manuscript.

## Funding

The research leading to these results received funding from Federal State Budgetary Institution, “Fund for Assistance to the Development of Small Forms of Enterprises in the scientific and technical field” (Fund for Assistance to Innovations) under Grant Agreement No. 18051ГV/2022.

## Acknowledgments

The work was carried out using the equipment of the center for collective use of the Lobachevsky University.

## References

- [1] Zhou, L.-Q.; Wang, J.-Y.; Yu, S.-Y.; Wu, G.-G.; Wei, Q.; Deng, Y.-B.; Wu, X.-L.; Cui, X.-W.; Dietrich, C.F. Artificial Intelligence in Medical Imaging of the Liver. *World J. Gastroenterol.* **2019**, *25*, 672–682. [\[CrossRef\]](#)
- [2] Żukowska, M.; Górski, F.; Bromiński, G. Rapid Manufacturing and Virtual Prototyping of Pre-Surgery Aids. In *World Congress on Medical Physics and Biomedical Engineering 2018*; Lhotska, L., Sukupova, L., Lacković, I., Ibbott, G.S., Eds.; IFMBE Proceedings; Springer Singapore: Singapore, 2018; Volume 68/3, pp. 399–403. [\[CrossRef\]](#)
- [3] Lanzarone, E.; Marconi, S.; Conti, M.; Auricchio, F.; Fassi, I.; Modica, F.; Pagano, C.; Pourabdollahian, G. Hospital Factory for Manufacturing Customised, Patient-Specific 3D Anatomic-Functional Models and Prostheses. In *Factories of the Future*; Tolio, T., Copani, G., Terkaj, W., Eds.; Springer International Publishing: Cham, Switzerland, 2019; pp. 233–254. [\[CrossRef\]](#)
- [4] Esposito Corcione, C.; Gervaso, F.; Scalera, F.; Padmanabhan, S.K.; Madaghiele, M.; Montagna, F.; Sanino, A.; Licciulli, A.; Maffezzoli, A. Highly Loaded Hydroxyapatite Microsphere/PLA Porous Scaffolds Obtained by Fused Deposition Modelling. *Ceram. Int.* **2019**, *45*, 2803–2810. [\[CrossRef\]](#)
- [5] Yadav, D.; Chhabra, D.; Kumar Garg, R.; Ahlawat, A.; Phogat, A. Optimization of FDM 3D Printing Process Parameters for Multi-Material Using Artificial Neural Network. *Mater. Today Proc.* **2020**, *21*, 1583–1591. [\[CrossRef\]](#)
- [6] Singh, R.; Singh, G.; Singh, J.; Kumar, R. Investigations for Tensile, Compressive and Morphological Properties of 3D Printed Functional Prototypes of PLA-PEKK-HAp-CS. *J. Thermoplast. Compos. Mater.* **2021**, *34*, 1408–1427. [\[CrossRef\]](#)
- [7] Li, J.; Li, L.; Zhou, J.; Zhou, Z.; Wu, X.; Wang, L.; Yao, Q. 3D Printed Dual-Functional Biomaterial with Self-Assembly Micro-Nano Surface and Enriched Nano Silver for Antibacterial and Bone Regeneration. *Appl. Mater. Today* **2019**, *17*, 206–215. [\[CrossRef\]](#)
- [8] Boonlaksiri, Y.; Prapagdee, B.; Sombatsompop, N. Promotion of Polylactic Acid Biodegradation by a Combined Addition of PLA-Degrading Bacterium and Nitrogen Source under Submerged and Soil Burial Conditions. *Polym. Degrad. Stab.* **2021**, *188*, 109562. [\[CrossRef\]](#)
- [9] Morettini, G.; Palmieri, M.; Capponi, L.; Landi, L. Comprehensive Characterization of Mechanical and Physical Properties of PLA Structures Printed by FFF-3D-Printing Process in Different Directions. *Prog. Addit. Manuf.* **2022**, *7*, 1111–1122. [\[CrossRef\]](#)
- [10] Taib, N.-A.A.B.; Rahman, M.R.; Huda, D.; Kuok, K.K.; Hamdan, S.; Bakri, M.K.B.; Julaihi, M.R.M.B.; Khan, A. A Review on Poly Lactic Acid (PLA) as a Biodegradable Polymer. *Polym. Bull.* **2023**, *80*, 1179–1213. [\[CrossRef\]](#)
- [11] Moetazedian, A.; Gleadall, A.; Han, X.; Silberschmidt, V.V. Effect of Environment on Mechanical Properties of 3D Printed Polylactide for Biomedical Applications. *J. Mech. Behav. Biomed. Mater.* **2020**, *102*, 103510. [\[CrossRef\]](#) [\[PubMed\]](#)
- [12] Castañeda-Rodríguez, S.; González-Torres, M.; Ribas-Aparicio, R.M.; Del Prado-Audelo, M.L.; Leyva-Gómez, G.; Gürrer, E.S.; Sharifi-Rad, J. Recent Advances in Modified Poly (Lactic Acid) as Tissue Engineering Materials. *J. Biol. Eng.* **2023**, *17*, 21. [\[CrossRef\]](#)
- [13] Alexeeva, O.V.; Olkhov, A.A.; Konstantinova, M.L.; Podmasterev, V.V.; Petrova, T.V.; Martirosyan, L.Y.; Karyagina, O.K.; Kozlov, S.S.; Lomakin, S.M.; Tretyakov, I.V.; et al. A Novel Approach for Glycero-(9,10-Trioxolane)-Trialeate Incorporation into Poly(Lactic Acid)/Poly(ε-Caprolactone) Blends for Biomedicine and Packaging. *Polymers* **2023**, *16*, 128. [\[CrossRef\]](#) [\[PubMed\]](#)
- [14] Mathur, V.; Agarwal, P.; Srinivasan, V.; Panwar, A.; Vasanthan, K. S. Facet of 4D Printing in Biomedicine. *J. Mater. Res.* **2023**, *38*, 2–18. [\[CrossRef\]](#)
- [15] Mohammadi-Zerankeshi, M.; Alizadeh, R. 3D-Printed PLA-Gr-Mg Composite Scaffolds for Bone Tissue Engineering Applications. *J. Mater. Res. Technol.* **2023**, *22*, 2440–2446. [\[CrossRef\]](#)
- [16] Pawłowska, A.; Stepczyńska, M.; Walczak, M. Flax Fibres Modified with a Natural Plant Agent Used as a Reinforcement for the Polylactide-Based Biocomposites. *Ind. Crops Prod.* **2022**, *184*, 115061. [\[CrossRef\]](#)
- [17] Yoon, S.-K.; Chung, D.-J. In Vivo Degradation Studies of PGA-PLA Block Copolymer and Their Histological Analysis for Spinal-Fixing Application. *Polymers* **2022**, *14*, 3322. [\[CrossRef\]](#) [\[PubMed\]](#)
- [18] Jiang, A.; Patel, R.; Padhan, B.; Palimkar, S.; Galgali, P.; Adhikari, A.; Varga, I.; Patel, M. Chitosan Based Biodegradable Composite for Antibacterial Food Packaging Application. *Polymers* **2023**, *15*, 2235. [\[CrossRef\]](#)



- [19] Khayrova, A.; Lopatin, S.; Varlamov, V. Black Soldier Fly *Hermetia Illucens* as a Novel Source of Chitin and Chitosan. *Int. J. Sci.* **2019**, *8*, 81–86. [[CrossRef](#)]
- [20] Terkula Iber, B.; Azman Kasan, N.; Torsabo, D.; Wese Omuwa, J. A Review of Various Sources of Chitin and Chitosan in Nature. *J. Renew. Mater.* **2022**, *10*, 1097–1123. [[CrossRef](#)]
- [21] Desai, N.; Rana, D.; Salave, S.; Gupta, R.; Patel, P.; Karunakaran, B.; Sharma, A.; Giri, J.; Benival, D.; Kommineni, N. Chitosan: A Potential Biopolymer in Drug Delivery and Biomedical Applications. *Pharmaceutics* **2023**, *15*, 1313. [[CrossRef](#)] [[PubMed](#)]
- [22] Chae, E.; Choi, S.-S. Analysis of Polymeric Components in Particulate Matter Using Pyrolysis-Gas Chromatography/Mass Spectrometry. *Polymers* **2022**, *14*, 3122. [[CrossRef](#)]
- [23] Fourie, J.; Taute, F.; Du Preez, L.; De Beer, D. Chitosan Composite Biomaterials for Bone Tissue Engineering—A Review. *Regen. Eng. Transl. Med.* **2022**, *8*, 1–21. [[CrossRef](#)]
- [24] Ressler, A. Chitosan-Based Biomaterials for Bone Tissue Engineering Applications: A Short Review. *Polymers* **2022**, *14*, 3430. [[CrossRef](#)] [[PubMed](#)]
- [25] Rezaei, F.S.; Khorshidian, A.; Beram, F.M.; Derakhshani, A.; Esmacili, J.; Barati, A. 3D Printed Chitosan/Polycaprolactone Scaffold for Lung Tissue Engineering: Hope to Be Useful for COVID-19 Studies. *RSC Adv.* **2021**, *11*, 19508–19520. [[CrossRef](#)] [[PubMed](#)]
- [26] Hamed, H.; Moradi, S.; Hudson, S.M.; Tonelli, A.E.; King, M.W. Chitosan Based Bioadhesives for Biomedical Applications: A Review. *Carbohydr. Polym.* **2022**, *282*, 119100. [[CrossRef](#)]
- [27] Zeng, S.; Ye, J.; Cui, Z.; Si, J.; Wang, Q.; Wang, X.; Peng, K.; Chen, W. Surface Biofunctionalization of Three-Dimensional Porous Poly(Lactic Acid) Scaffold Using Chitosan/OGP Coating for Bone Tissue Engineering. *Mater. Sci. Eng. C* **2017**, *77*, 92–101. [[CrossRef](#)]
- [28] Xu, Z.; Wang, N.; Liu, P.; Sun, Y.; Wang, Y.; Fei, F.; Zhang, S.; Zheng, J.; Han, B. Poly(Dopamine) Coating on 3D-Printed Poly-Lactic-Co-Glycolic Acid/ $\beta$ -Tricalcium Phosphate Scaffolds for Bone Tissue Engineering. *Molecules* **2019**, *24*, 4397. [[CrossRef](#)] [[PubMed](#)]
- [29] Abifar, J.K.; Prakash, C.; Singh, S. Optimization and Significance of Fabrication Parameters on the Mechanical Properties of 3D Printed Chitosan/PLA Scaffold. *Mater. Today Proc.* **2022**, *50*, 2018–2025. [[CrossRef](#)]
- [30] Lednev, I.; Salomatina, E.; Ilyina, S.; Zaitsev, S.; Kovylin, R.; Smirnova, L. Development of Biodegradable Polymer Blends Based on Chitosan and Polylactide and Study of Their Properties. *Materials* **2021**, *14*, 4900. [[CrossRef](#)]
- [31] Kaliva, M.; Georgopoulou, A.; Dragatogiannis, D.A.; Charitidis, C.A.; Chatzinikolaidou, M.; Vamvakaki, M. Biodegradable Chitosan-Graft-Poly(L-Lactide) Copolymers For Bone Tissue Engineering. *Polymers* **2020**, *12*, 316. [[CrossRef](#)]
- [32] Rojas-Martínez, L.E.; Flores-Hernández, C.G.; López-Marín, L.M.; Martínez-Hernández, A.L.; Thorat, S.B.; Reyes Vázquez, C.D.; Del Río-Castillo, A.E.; Velasco-Santos, C. 3D Printing of PLA Composites Scaffolds Reinforced with Keratin and Chitosan: Effect of Geometry and Structure. *Eur. Polym. J.* **2020**, *141*, 110088. [[CrossRef](#)]
- [33] Osman, M.A.; Virgilio, N.; Rouabhia, M.; Mighri, F. Development and Characterization of Functional Polylactic Acid/Chitosan Porous Scaffolds for Bone Tissue Engineering. *Polymers* **2022**, *14*, 5079. [[CrossRef](#)] [[PubMed](#)]
- [34] Hien NT, T.; Trinh, T.N.; Long, H.B.; Ha Cam, A.; Huynh Dai, P. Characterization of Electrospayed Chitosan/PLA-PEG-PLA (Copolymer) Nanoparticles for Encapsulation of Hydrophilic Drug. *Vietnam J. Sci. Technol.* **2022**, *60*, 436–446. [[CrossRef](#)]
- [35] Shakola, T.V.; Rubanik, V.V.; Rubanik, V.V., Jr.; Kurliuk, A.V.; Kirichuk, A.A.; Tskhovrebov, A.G.; Egorov, A.R.; Kritchenkov, A.S. The First Electrochemical N-Arylation of Chitosan. Antibacterial Effect of Novel Cationic Chitosan Derivatives. *Eur. Polym. J.* **2023**, *198*, 112418. [[CrossRef](#)]
- [36] Lammens, N.; Kersemans, M.; Luyckx, G.; Van Paepegem, W.; Degrieck, J. Improved Accuracy in the Determination of Flexural Rigidity of Textile Fabrics by the Peirce Cantilever Test (ASTM D1388). *Text. Res. J.* **2014**, *84*, 1307–1314. [[CrossRef](#)]
- [37] Mertz, A.M.; Mix, A.W.; Baek, H.M.; Giacomini, A.J. Understanding Melt Index and ASTM D1238. *J. Test. Eval.* **2013**, *41*, 20120161. [[CrossRef](#)]
- [38] Ghazalian, M.; Afshar, S.; Rostami, A.; Rashedi, S.; Bahrami, S.H. Fabrication and Characterization of Chitosan-Polycaprolactone Core-Shell Nanofibers Containing Tetracycline Hydrochloride. *Colloids Surf. A Physicochem. Eng. Asp.* **2022**, *636*, 128163. [[CrossRef](#)]